NMPC USING PONTRYAGIN'S MINIMUM PRINCIPLE -- APPLICATION TO A TWO-PHASE SEMI-BATCH HYDROFORMYLATION REACTOR UNDER UNCERTAINTY

Erdal Aydin [a,b], Dominique Bonvin [c], Kai Sundmacher [a,d,*]

[a]*Max Planck Institute for Dynamics of Complex Technical Systems, Sandtorstraße 1, 39106 Magdeburg, Germany*

[b]*International Max Planck Research School (IMPRS) for Advanced Methods in Process and Systems Engineering, Magdeburg, Germany*

[c]*Laboratoire d'Automatique, Ecole Polytechnique Fédérale de Lausanne, CH-1015 Lausanne, Switzerland*

[d]*Otto-von-Guericke University Magdeburg, Universitätplatz 2, 39106 Magdeburg, Germany*

* Corresponding author: sundmacher@mpi-magdeburg.mpg.de ; Tel: +49 391 6110 350, Fax: +49 391 6110 353

ABSTRACT

Nonlinear model predictive control (NMPC) is an important tool to perform real-time optimization for batch and semi-batch processes. Direct methods are often the methods of choice to solve the corresponding optimal control problems, in particular for large-scale problems. However, the matrix factorizations associated with large prediction horizons can be computationally demanding. In contrast, indirect methods can be competitive for smaller-scale problems. Furthermore, the interplay between states and co-states in the context of Pontryagin's Minimum Principle might turn out to be computationally quite efficient.

This work proposes to use an indirect solution technique within shrinking-horizon in the context of NMPC. In particular, the technique deals with path constraints via indirect adjoining, which allows meeting active path constraints explicitly at each iteration. Uncertainties are handled by the introduction of time-varying backoff terms for the path

constraints. The resulting NMPC algorithm is applied to a two-phase semi-batch reactor for the hydroformylation of 1-dodecene in the presence of uncertainty, and its performance is compared to that of NMPC that uses a direct simultaneous optimization method. The results show that the proposed algorithm (i) can enforce feasible operation for different uncertainty realizations both within batch or from batch to batch, and (ii) it is significantly faster than direct simultaneous NMPC, especially at the beginning of the batch. In addition, a modification of the PMP-based NMPC scheme is proposed that enforces active constraints via tracking.

Keywords: Nonlinear model predictive control, indirect optimization methods, semi-batch processes, Pontryagin's Minimum Principle, shrinking-horizon NMPC

1. Introduction

Batch and semi-batch processes have wide application in the specialty industries for the production of low-volume, high-added-value products. Typical examples are pharmaceuticals, polymers and food. With increasing competition in industry and stricter environmental regulations, the optimal operation of batch processes plays an important role toward increased profitability. The inherently transient behavior as well as the presence of strong nonlinearities and of path and end-point constraints result in challenging optimization problems. Moreover, the lack of accurate models brings about considerable plant-model mismatch (Terwiesch et al., 1994; Bonvin, 1998; Srinivasan et al., 2003b; Jung et al., 2015). Hence, the open-loop implementation of off-line computed optimal control profiles may result in sub-optimal, or worse, infeasible operation. In addition, the operation conditions might change from batch to batch and cause unacceptable variations on product quality. Consequently, the application of measurement-based, optimizing feedback schemes is of great importance for semi-batch processes (Eaton and Rawlings, 1990; Ruppen et al., 1995; Ruppen et al., 1998; Bonvin et al., 2001; Bonvin, 2006; Kadam et al., 2007; Welz et al., 2008; Mesbah et al., 2011)

Model predictive controllers (MPC) have been used extensively in industry (García et al., 1989; Qin and Badgwell, 2003). On the basis of a (most often linear) process model, these controllers predict the future behavior of the states and outputs. At each iteration, the algorithm updates the initial conditions using measurements and solves a dynamic optimization problem for some cost function such as the minimization of a tracking stage cost or the maximization of a final cost. Only the first part of the computed optimal inputs is implemented, then the horizon is shifted by one sampling time and the procedure is repeated recursively. Since MPC is capable of addressing multivariable constrained nonlinear systems and can use different types of models and performance criteria, it possesses a suitable and flexible structure for real-time optimizing control (Diehl et al., 2002; Adetola and Guay, 2010;

De Souza et al., 2010; Huang et al., 2010). A detailed discussion and survey on MPC can be found in (Morari and Lee, 1999).

Because of the strong nonlinear behavior of batch processes, linear MPC is often not the method of choice for batch and semi-batch processes. Moreover, semi-batch processes usually require strict constrained operation since the ability to influence the performance and feasibility of the process decreases with time (Bonvin, 1998). This motivates the use of shrinking-horizon nonlinear model predictive controllers (NMPC), for which the optimization is performed with respect to the full time horizon and includes both path and terminal constraints (Nagy and Braatz, 2003; Nagy et al., 2007).

Several studies on the applicability of NMPC to batch processes have been reported in the literature. (Lakshmanan and Arkun, 1999) used linear parameter-varying models for the estimation and control of nonlinear batch processes. (Seki et al., 2001) proposed an NMPC structure for the industrial application on polymerization reactors. (Nagy and Braatz, 2003) studied a robust NMPC scheme for batch crystallization, whereby parametric uncertainties were taken into account explicitly. (Valappil and Georgakis, 2002) suggested a min-max NMPC scheme with successive linearization for the control of the end-point properties in batch reactors. (Lucia et al., 2013) suggested a multi-stage NMPC scheme to deal with uncertainties, and a scenario-tree approach was used to optimize a semi-batch polymerization reactor. Recently, (Jang et al., 2016) proposed a multi-stage NMPC scheme for semi-batch reactors using backoffs on path constraints. (Binette and Srinivasan, 2016) compared the performance of different tracking objectives for the NMPC of batch processes without parameters adaptation.

Nonlinear dynamic optimization (or optimal control) is at the core of NMPC and plays an important role in terms of implementation. Both the complexity and the computational time of the model-based optimizing controllers are of great concern and must consider the time

available for sampling and the possible presence of feedback delays (Misik et al., 2016). The solution methods for dynamic optimization problems fall into the category of direct and indirect methods (Srinivasan et al., 2003b).

Direct methods: In direct sequential methods, the input vector is parameterized using polynomial functions, the states are integrated from their current values up to the final time, and the optimal input parameters are determined by a NLP solver (Vassiliadis et al., 1994; Srinivasan et al., 2003b). Since the states are not approximated, these methods are called 'feasible-path' methods. The computational complexity might turn out to be high, in particular for path-constrained problems, which is usually not acceptable for real-time algorithms.

In direct simultaneous methods (DSM), the optimal control problem is transformed to a NLP upon discretizing both the inputs and the states. Since the states are approximated instead of integrated, these approaches are called 'infeasible-path' methods. Direct simultaneous methods were reported to be effective for large-scale optimization and continuous NMPC problems in the literature (Cervantes and Biegler, 1998; Biegler et al., 2002; Wächter and Biegler, 2006; Kameswaran and Biegler, 2006; Biegler, 2007; Huang et al., 2009; Jang et al., 2016). (Zavala and Biegler, 2009) introduced an 'advanced-step' DSM to deal with the feedback delay associated with the time required to compute the solution. Later, (Huang et al., 2010) extended this method for the combination of NMPC and moving horizon estimation.

Another direct solution algorithm proposed for NMPC is the direct multiple shooting which represents a mid-way between sequential and simultaneous algorithms. In these methods, the time interval is divided into stages and the initial conditions of the stages are taken as decision variables for the optimization problem. This procedure is also an 'infeasible-path' method but the integration is as accurate as in sequential methods

(Srinivasan et al., 2003b). Direct multiple shooting has been used extensively in NMPC problems (Keil, 1999; Bock et al., 2000; Diehl et al., 2002; Diehl et al., 2006; Schäfer et al., 2007; Findeisen et al., 2007). (Mesbah et al., 2011) compared the performance of the DSM and direct multiple shooting algorithms for the real-time control of a fed-batch crystallizer.

Indirect methods: In indirect optimization methods, the optimization problem is reformulated as the minimization of an Hamiltonian function (Bryson, 1975). The reformulated problem is then solved to satisfy the necessary conditions of optimality (NCO) using Pontryagin's Minimum Principle (PMP). Indirect methods have been used to solve MPC problems in the literature. (Cannon et al., 2008) designed a MPC strategy for input-constrained linear systems, where the inputs can be represented in terms of co-states and the problem is solved using active-set methods. It was stated that the matrix factorizations performed by general direct solvers can be efficiently replaced by the computation of the states and co-states using PMP. This way, the complexity per iteration increases only linearly with the length of the prediction horizon, which can be a computational advantage for batch processes that typically have large prediction horizons due to the shrinking-horizon approach. (Kim and Rousseau, 2012) used PMP for the optimal control of hybrid electric vehicles. (Ali and Wardi, 2015) proposed a multiple shooting method based on PMP, where the inputs can be expressed analytically in terms of states and co-states. Recently, (Zhang et al., 2017) applied PMP in the MPC of a plug-in vehicle. In this method, the values of the co-states are determined by trial and error. For a more detailed review on the solution algorithms for NMPC, the reader is referred to (Cannon, 2004).

However, until very recently (Aydin et al., 2017), there did not exist a fast convergent method to solve path-constrained optimal control problems using PMP (Hartl et al., 1995;

Chachuat, 2007). Aydin et al. (2017) proposed an indirect, gradient-based dynamic optimization algorithm for the control of non-affine constrained semi-batch processes. The algorithm uses indirect adjoining to deal with path constraints, which allows the explicit calculation of inputs to meet the path constraints at each iteration step. The performance of PMP-based and DSM-based algorithms was compared on three different problems, with the indirect algorithm being found to be computationally superior, especially with finer discretization levels. In this work, we apply the convergent PMP-based algorithm proposed by Aydin et al. (2017) to the constrained NMPC problem of batch processes with both mixed and pure-state path constraints.

Tracking the necessary conditions of optimality (NCO tracking) has also been studied as a real-time optimization algorithm (Srinivasan & Bonvin, 2007). The optimal inputs are first computed via off-line optimization of the nominal model. The main assumption is that the solution structure (sequence and types of arcs) does not change with uncertainty. Hence, instead of performing explicit optimization at each NMPC iteration, the optimal solution structure computed off-line is tracked with the help of feedback controllers (Srinivasan and Bonvin, 2007; Srinivasan et al., 2008; Chachuat et al., 2009; Ebrahim et al., 2016).

The computational advantage of the PMP formulation represents the main motivation for this study. We propose to apply the novel PMP-based solution algorithm (Aydin et al., 2017) to the shrinking-horizon NMPC of *nonlinear* semi-batch processes in the presence of nonlinear pure and mixed state path constraints. The effect of uncertainties will be handled by the introduction of time-varying backoffs (Visser et al., 2000; Srinivasan et al., 2003a; Shi et al., 2016).

The paper is organized as follows. Section 2 presents the indirect solution algorithm and its application to NMPC. Section 3 illustrates the proposed method via the case study of a two-phase semi-batch reactor for an hydroformylation process and compares its performance

with a DSM algorithm. Furthermore, the PMP-based algorithm is extended to the case where active constraints are enforced via tracking. Finally, Section 4 concludes the study.

2. NMPC Problem and Solution Algorithm

In NMPC of semi-batch processes, the optimal control problem to be solved on-line at each iteration can be written as follows:

$$\begin{aligned} &\min_{u(t)} J = \phi(x(t_f, \theta)) \\ \text{s.t.} \quad &\dot{x} = F(x, u, \theta), \quad x(t_k) = x_{t_k} \\ &S(x, u, \theta) \leq 0, \quad T(x(t_f), \theta) \leq 0, \quad t \in [t_k, t_f] \end{aligned} \tag{1}$$

where t_k is the *k*-th sampling time, *J* is a scalar performance index that depends on the values of the states at the final time t_f, ϕ is the objective function, *x* is the n_x-dimensional state vector with the corresponding initial conditions $x(t_k)$, u is the n_u-dimensional input vector, *S* is the n_S-dimensional vector of inequality path constraints that include input bounds, *T* is the n_T-dimensional vector of inequality terminal constraints, and θ is the vector of uncertain parameters associated with plant-model mismatch. After solving Problem (1), the first part $u[t_k, t_k + \delta]$ of the optimal inputs is implemented in the plant, the horizon is shrunk by the sampling interval δ, and a new optimal control problem is solved. This procedure is repeated recursively until the final batch time is reached.

Several methods are available in the literature to cope with uncertainties in the context of stochastic programming or two-level approaches (Sahinidis, 2004; Li et al., 2008; Mesbah et al., 2014; Puschke et al., 2016; Mesbah, 2016; Puschke and Mitsos, 2016). However, the computational time associated with these methods is still a limitation for real-time optimization and thus these methods are out of the scope of this study. To deal with the effect of uncertainties, we introduce here time-varying backoffs (Visser et al., 2000; Srinivasan et al., 2003a; Shi et al., 2016). Furthermore, it is assumed that x_{t_k} can be measured or estimated with negligible time delay using on-line sensors and state estimation (Allgöwer et al., 1999; Rao et al., 2001; Rao and Rawlings, 2002; Schneider and Georgakis, 2013). Using small

sampling times and frequent on-line measurements, the conservatism associated with the robust backoff approach can be reduced.

The optimal control problem given in Eq. 1 can be reformulated using PMP and the constraint backoffs as follows:

$$\min_{u(t)} H(t) = \lambda^T F(x,u,\theta_0) + \mu^T[S(x,u,\theta_0) + b_s]$$

$$\text{s.t.} \quad \dot{x} = F(x,u,\theta_0); \quad x(t_k) = x_{t_k};\ t \in [t_k, t_f]$$

$$\dot{\lambda}^T = -\frac{\partial H}{\partial x}, \quad \lambda^T(t_f) = \frac{\partial \phi}{\partial x}\Big|_{t_f} + \upsilon^T \frac{\partial T}{\partial x}\Big|_{t_f};$$

$$\mu^T[S(x,u,\theta_0) + b_s] = 0; \quad \upsilon^T[T(x(t_f),\theta_0) + b_T] = 0$$

$$\frac{\partial H(t)}{\partial u} = \lambda^T \frac{\partial F}{\partial u} + \mu^T \frac{\partial S}{\partial u} = 0 \tag{2}$$

where H is the Hamiltonian function, θ_0 is the nominal value of the parameters, λ is the n_x-dimensional vector of Lagrange multipliers (also called co-states or adjoints) for the system equations, μ is the n_S-dimensional vector of Lagrange multipliers for the path constraints, and υ is the n_T-dimensional vector of Lagrange multipliers for the terminal constraints, b_s and b_T are the backoffs associated with the path and terminal constraints, respectively. The terms $\mu^T[S(x,u,\theta_0) + b_s] = 0$ and $\upsilon^T[T(x(t_f),\theta_0) + b_T]$ are the complementary slackness conditions that will be satisfied at the optimum. Additionally, the partial derivatives of the Hamiltonian function with respect to the inputs must all be equal to zero at an optimum.

To initialize the solution algorithm, the problem should be cast as the solution to the differential equations for both the states and the co-states. This is done by differentiating the Hamiltonian function with respect to the states, as given in Eq. 2. The Matlab Symbolic Toolbox can be used for this purpose. The input profiles are discretized as *u*(t) = `U`*(U)*, where *U* is a (n_u x *N*) matrix that contains *N* discrete input values for the n_u inputs. Note that *U* could

be initialized using the nominal optimal solution. Furthermore, the Lagrange multipliers for the path constraints are also discretized as μ (t) = M (*M*), where *M* is a (n_S x *N*) matrix.

Indirect adjoining can be used to deal with pure-state path constraints of the form $S(x, \theta_0) + b_s \leq 0$. The state constraints are differentiated with respect to time until at least one of the inputs appears explicitly (Hartl et al., 1995; Aydin et al., 2017). The resulting expression is $S^{\{n\}}(x,u,\theta_0) \leq 0$, where *n* represents the relative degree of a constraint with respect to an input, that is, the number of differentiations required for an input to appear explicitly (Srinivasan and Bonvin, 2007). Then, the differentiated version $S^{\{n\}}(x,u,\theta_0) \leq 0$ is used to construct the new Hamiltonian H′. Due to the complementary slackness, the penalty term $\mu^T[S(x, u, \theta_0) + b_s] = 0$ vanishes when all the constraints are satisfied. Nevertheless, if some of the constraints cannot be indirectly adjoined, the penalty term $\mu^T S(x) = K$ will force convergence to occur through the feasible region (Onori et al., 2016). The idea of indirect adjoining and constraint activation is illustrated in Fig. 1.

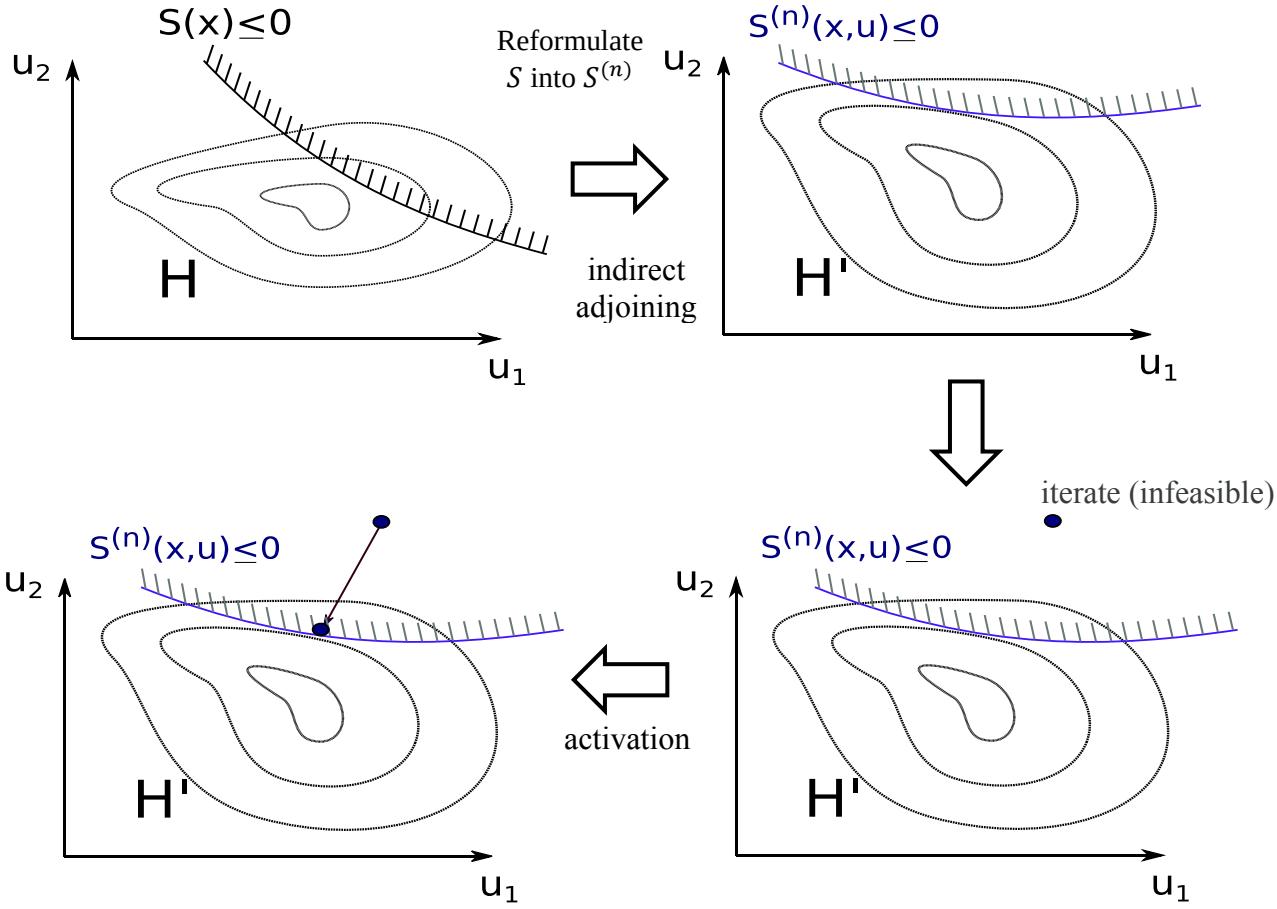

Figure 1. Indirect adjoining and constraint activation.

Assuming that the system and adjoint equations are differentiable, the algorithmic steps proposed for solving the problem given in Eq. 2 can be summarized as follows (Aydin et al., 2017):

PMP-based Solution Algorithm

Select values for the penalty term K, the step size α, the coefficient β, the threshold ε, the number of discrete input values N, the maximum number of iterations *iter_max*, and the backoff b_s. Initialize the iteration counter $h = 0$ and the corresponding input elements U_0 and Hessian matrix $B_0 := \boldsymbol{I}$.

do $h = 1 \rightarrow$ *iter_max*

I. Solve the state equations by forward integration and the co-state equations by backward integration. If the j-th constraint is satisfied at the discrete time instant k, set M_h (j,k) $:= 0$. Otherwise, set M_h (j,k) $:= K > 0$, for k=1,..,N.

II. Evaluate the value of the first-order gradients $(\frac{\partial H}{\partial U})_h$ by using pre-computed analytical expressions.

III. **If** all constraints are satisfied, set $U_{h+1} := U_h - \alpha(B_h{}^{-1}\frac{\partial H}{\partial U})_h$ and update the Hessian matrix B_h as follows:

$y := \nabla H(U_{h+1}) - \nabla H(U_h)$, $s := U_{h+1} - U_h$,

if $s^T y \geq \beta\|s\|^2$, set $B_{h+1} := B_h + \frac{yy^T}{s^T y} - \frac{B_h s s^T B_h}{s^T B_h s}$,

else set $B_{h+1} := B_h$

end if

else set $U_{h+1} := U_h - \alpha(\frac{\partial H}{\partial U})_h$ and $B_{h+1} := B_h$, and compute the value of $U(.,k)$ that makes the violated path constraint $S_j^{\{n\}}(x, U(.,k)) + b_s = 0$ at the discrete time instant k.

end if

IV. **If** $\left\|\frac{\partial H}{\partial U}\right\|_h < \varepsilon$, set $U_{opt} := U_h$, stop, **end if**

end **do**

Remark 1. Input constraint saturation is implemented such that

$$u(t) = \begin{cases} u_{min}, & \text{if a lower constraint is violated} \\ u_{max}, & \text{if an upper constraint is violated} \end{cases}$$

Remark 2. Closed-loop stability can be enforced by adding an extra terminal cost or constraint to the problem (García et al., 1989; Diehl et al., 2011; Angeli et al., 2012), which comes as an additional advantage of the proposed algorithm compared to other indirect methods (Cannon et al., 2008).

Remark 3. To speed-up the real-time algorithm, NMPC is initialized with the open-loop optimal control profiles as initial guesses. After each iteration, when the horizon shrinks, the previous optimal profiles are interpolated linearly with respect to the new horizon and serve as initial guesses for the next optimization.

Remark 4. Since the proposed algorithm searches for a feasible point at each iteration, it can be implemented in a sub-optimal fashion by setting a minimal number of iterations to further reduce the computational effort (Findeisen et al., 2007).

3. Case Study: Two-phase Semi-batch Hydroformylation Reactor

3.1 Problem Formulation

Due to their chemical nature, long-chain olefins are potential renewable feedstock to be integrated into existing petrochemical production networks. Hydroformylation is a suitable way of converting these feedstocks into valuable intermediates like aldehydes. A carbon double bond can be converted into an aldehyde group with the addition of H_2 and CO in hydroformylation using an homogeneous catalyst (Hentschel et al., 2015; Kaiser et al., 2016).

Consider the semi-batch operation of hydroformylation in a two-phase stirred-tank reactor. The objective is to maximize the final concentration of n-tridecanal (nC13al) from 1-dodecene (nC12en) that reacts with syngas ($H_2 + CO$). The final time is fixed at 70 min. The reaction network is illustrated in Fig. 2 (Hentschel et al., 2015).

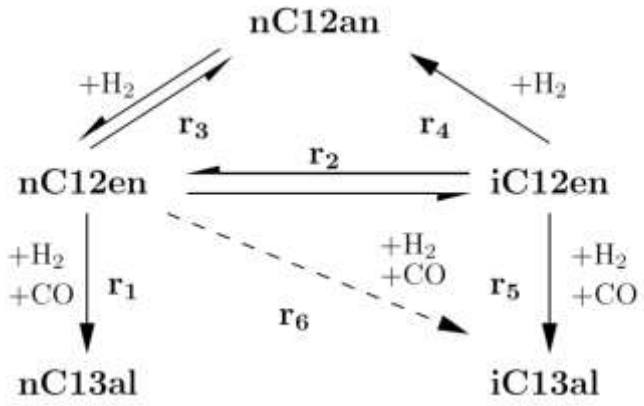

Figure 2. Hydroformylation reaction network.

The input variables are the reactor temperature $T(t)$ and the feedrate $u(t)$ of syngas. Equimolar content of *CO* and H_2 in the syngas is assumed. The gas and liquid phases are modeled as ideally mixed phases. The model parameters have been identified and validated using experimental data (Hentschel et al., 2015). In addition to bounds on the input variables, the total pressure of the gas phase must be kept within specified limits. It is seen from the model that the first time derivative of the total pressure contains the input $u(t)$ explicitly, thus

implying a relative degree 1 for this constraint. As a result, this constraint can be indirectly adjoined into the Hamiltonian and will be activated at each infeasible iteration as illustrated in Fig. 1.

Including the backoff term b_s, the optimal control problem to be solved on-line at each NMPC iteration is as follows:

$$\max_{u(t),T(t)} J = c_{nc13al}(t_f) \qquad t \in [t_k, t_f]$$

$$\text{s.t} \qquad \dot{c}_{liq,i} = {j_i}^{GL} + c_{cat} M_{cat} \sum_{j\in\mathbb{R}} v_{j,i} r_j \; ; \quad c_{liq,i}(t_k) = \hat{c}_{liq,i,t_k}; \quad \text{i=1, 2,…,7;}$$

$$\dot{p}_i = \frac{RT}{V_{gas}}\left(u\, x_i - V_{liq}\, {j_i}^{GL}\right) \;\; (i \in gas) \; ; \;\; p_i(t_k) = p_{i,t_k} \; ; \;\; x_i \;=\; 0.5 \left(\frac{\text{mol}}{\text{mol}}\right); \;\; \text{i} = 1, 2;$$

$${j_i}^{GL} = \begin{cases} (k_L a)_i \left(c_i{}^* - c_{liq,i}\right), & (if\ i \in gas); \quad \text{i} = 1, 2 \\ 0, & (else); \quad \text{i} = 3,4, \ldots, 7 \end{cases};$$

$$r_1 = \frac{k_{1,0}(T) c_{nC12en} c_{H_2} c_{CO}}{1 + K_{1,1} c_{nC12en} + K_{1,2} c_{nC13al} + K_{1,3} c_{H_2}} \; ;$$

$$r_2 = \frac{k_{2,0}(T)(c_{nC12en} - \frac{c_{iC12en}}{K_{p,2}})}{1 + K_{2,1} c_{nC12en} + K_{2,2} c_{iC12en}} \; ;$$

$$r_3 = \frac{k_{3,0}(T)(c_{nC12en} c_{H_2} - \frac{c_{nC12an}}{K_{p,3}})}{1 + K_{3,1} c_{nC12en} + K_{3,2} c_{nC13an} + K_{3,3} c_{H_2}} \; ;$$

$$r_4 = k_{4,0}(T) c_{iC12en} c_{H_2} \; ;$$

$$r_5 = k_{5,0}(T) c_{iC12en} c_{H_2} c_{CO} \; ;$$

$$r_6 = k_{6,0}(T) c_{nC12en} c_{H_2} c_{CO} \; ;$$

$$k_j(T) = k_{0,j} \exp\left(-\frac{E_{A,j}}{R}\left(\frac{1}{T} - \frac{1}{T_{ref}}\right)\right) \; ;$$

$$K_{p,j} = \exp\left(\frac{-\Delta G_j}{RT}\right);$$

$$-\Delta G_j = a_{0,j} + a_{1,j} T + a_{2,j} T^2 \; ;$$

$$c_{cat} = \frac{\gamma c_{cat,tot}}{1 + K_{cat,1} {c_{CO}}^{K_{cat,3}} + K_{cat,2} \frac{{c_{CO}}^{K_{cat,3}}}{c_{H_2}}} ;$$

$$c_i^* = \frac{p_i}{H_i} ;$$

$$H_i = {H_i}^0 \exp\left(\frac{-E_{A,H,i}}{RT}\right);$$

$$p_{total}(t) = p_{H_2}(t) + p_{CO}(t) ;$$

$$1\ bar \leq p_{total}(t) \leq 20\ bar - b_s(t);$$

$$0\ \text{mol/min} \leq u(t) \leq 7\ \text{mol/min};$$

$$368.15\ \text{K} \leq T(t) \leq 388.15\ \text{K}$$

$$\frac{|T(t) - T(t_k)|}{t - t_k} \leq \Delta T_{max}$$

$$c_{nc13al}(t_f) \leq 0.8 \qquad (3)$$

where t_k is the time at the *k*-th sampling instant, *i* represents the component index (i=1,2,…,7 for the liquid phase and i=1,2 for the gas phase), *j* stands for the reaction index and R is the reaction set, $\hat{c}_{liq,i,t_k}$ is the estimated concentration of the component *i* in the liquid phase, p_{i,t_k} is the measured pressure in the gas phase, γ is catalyst activity, b_s is the time-varying backoff associated with the pressure upper limit, whose value can be calculated by open-loop Monte Carlo simulations (Shi et al., 2016). The liquid volume V_{liq} and the gas volume V_{gas} inside the reactor are assumed constant (900 mL each). The nominal parameters θ_0 are given in (Hentschel et al., 2015). The total partial pressure and the concentration of each species are assumed to be measured at each NMPC iteration, e.g. using an on-line IR spectroscopy. A terminal constraint on the final value of the desired product ($c_{nc13al}(t_f) \leq 0.8$) is added to enforce closed-loop stability.

The optimal reactor temperature calculated by NMPC serves as set point for a thermostat, where a PID controller regulates the reactor temperature by adjusting the flow rate of heating/cooling fluid. Hence, a rate constraint on the temperature change is introduced (ΔT_{max}) so that the controller is capable of reaching the set point before the next NMPC

iteration. This rate constraint term depends on the heating/cooling capacity of the thermostat. On the other hand, the optimal feed flow rate can be implemented directly (Abel et al., 2000; Abel and Marquardt, 2003). It was observed that a relatively fine input discretization (N≥100) is necessary to get accurate and feasible optimal results, especially with regard to the pressure constraint (Aydin et al., 2017).

3.2 Estimation of Time-varying Backoffs

Backoffs are useful to enforce feasibility. The conservative nature of backoffs is reduced through the use of small sampling times. For choosing the backoff term b_s, the multi-step approach of (Shi et al., 2016) is used here. First, the nominal optimal input profiles are computed. This was done in (Aydin et al., 2017). Then, Monte-Carlo simulations are performed by sampling various uncertainties and using the optimal inputs in an open-loop manner. Finally, a time-varying backoff is determined from the standard deviation of constraint violations. Note that the Monte-Carlo approach might require a significant computational effort in the presence of multiple uncertainties, but this work is done offline.

In this study, the rate constants $k_{i,0}$ and the catalyst activity γ are assumed to vary within a certain range from batch to batch operation according to a uniform distribution. On the other hand, the gas-liquid mass-transfer coefficients $(k_L a)_i$ are assumed to vary within the batch. The uncertainty ranges for the parameters are given in Table 1. The results of open-loop Monte Carlo simulations for 40 realizations of multiple uncertainties are depicted in Fig. 3.

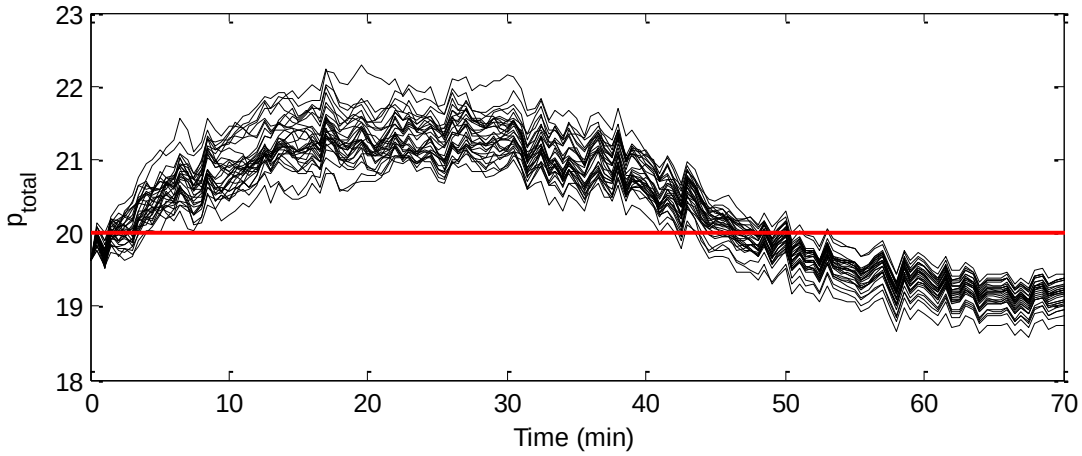

Figure 3a. Open-loop Monte Carlo simulations of total pressure for 40 uncertainty realizations.

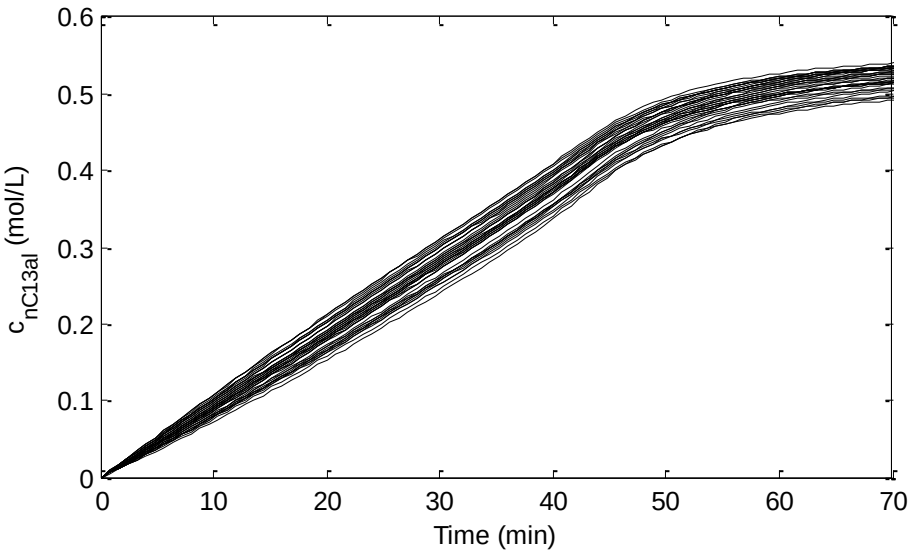

Figure 3b. Open-loop Monte Carlo simulations for the desired product concentration for 40 uncertainty realizations.

Table 1. Parameter variations for the hydroformylation process: $(k_L a)_i$ vary within batch, while $k_{i,0}$ and γ vary from batch to batch.

Parameter	Nominal Value (Hentschel et al., 2015)	Minimum Value	Maximum Value
$(k_L a)_1$	9.57	8.0	10.1
$(k_L a)_2$	7.08	5.5	7.6
$k_{1,0}$	4.904	2.9	5.2
$k_{2,0}$	4.878	3.8	5.8
$k_{3,0}$	2.724	1.7	3.7
$k_{4,0}$	2.958	1.9	3.9
$k_{5,0}$	3.702	2.7	4.7
$k_{6,0}$	3.951	2.9	4.9
γ	-	80 %	100 %

Accordingly, the time-varying backoff is chosen as follows:

$$b_s(t) = \begin{cases} 1.3 & if\ t \leq 30 \\ 0.7 & if\ 30 < t \leq\ 55 \\ 0 & if\ t > 55 \end{cases}$$

Remark 5. The backoff values can also be updated on a batch-to-batch manner so as to increase the performance of future batches.

3.3 NMPC for Product Maximization

The PMP-based solution algorithm for the NMPC was implemented in the Matlab environment. The DSM-based algorithm used the CasADI toolbox (Andersson and Diehl, 2012) that implements the Ipopt solver (Wächter and Biegler, 2006). All computational results

(excluding the initializations of the problems) were obtained using an Intel i-3-2100 machine (CPU 3.10 GHz 4 GB RAM). The tuning parameters for the PMP-based and the DSM-based algorithms are summarized in Table 2.

Table 2. Tuning parameters for the PMP-based and DSM-based algorithms.

PMP-based Algorithm	DSM-based Algorithm with Ipopt
sampling time = 15 s measurement frequency = 30 s measurement delay = 5 s α = 0.05; β = 0.1; ε = 0.01; N =100; K=20; iter_max =15 ΔT_{max}= (0.35 K)/(15s)	sampling time = 15 s measurement frequency = 30 s measurement delay = 5 s N =100; ipopt.max_iter = 100; ipopt.tol = 1e-4; ipopt.mu_init = 1e-6 ΔT_{max}= (0.35 K)/(15s)

The input profiles computed off-line using the nominal model are used as initial guesses at the beginning of the batch for both algorithms. Later, the optimal inputs computed at a given iteration are used to generate by interpolation the initial guesses for the next optimization.

All measurements are corrupted with white noise. Because the sampling times of the measurements and of the controller are not the same and, in addition, there is an inevitable measurement delay, an observer is designed to estimate the concentrations in the liquid phase using the model equations and a linear update term such that:

$$\begin{aligned} \hat{x}_k &= \int_{t_{k-1}}^{t_k} f(\hat{x}, u)dt + d_{k-1} \\ d_k &= L(x_k - \hat{x}_k) \end{aligned} \tag{4}$$

where d_k is the linear update term, $\hat{x}_k = \hat{c}_{liq,t_k}$, x_k are the measured states, $\hat{x}_k$ are the estimated states and $L = [0.75\ 0.75\ 0.65\ 0.75\ 0.75\ 0.75\ 0.75]^{\mathrm{T}}$ is the observer gain vector. All concentrations in the liquid phase are assumed to be measured every 30 sec (+ 5 sec delay) using an on-line FTIR, and the total pressure in the gas phase is assumed to be measured

every second with no delay. The NMPC algorithm takes into account the estimated states at each sampling time as the initial condition of the optimal control problem and the linear term d_k is updated as soon as the new measurements are obtained. The performance of the observer for a closed-loop batch is given in Fig. 4.

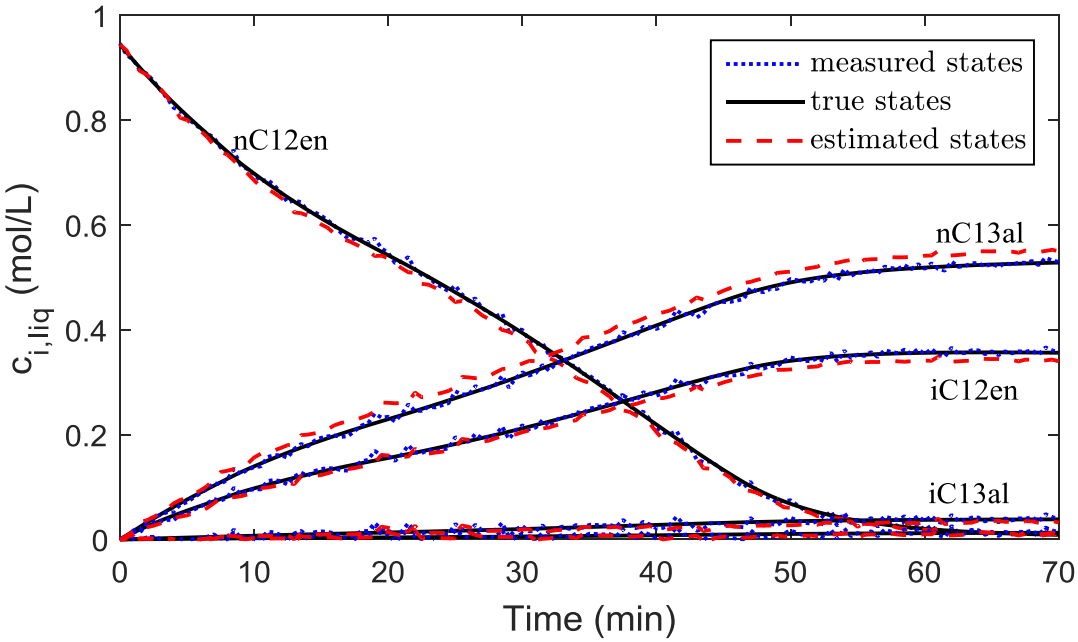

Figure 4. Performance of the observer for a single batch.

The performance of the DSM-based and PMP-based algorithms for the same disturbance realizations within a batch are compared in Fig. 5. The corresponding computational times for the individual iterations are given in Fig. 6. Because the total pressure can be measured in real-time without delay and taken into account by the NMPC algorithm, slight variations between the true and estimated concentrations do not affect the feasibility of the closed-loop process. Nevertheless, better state estimation might increase the cost performance.

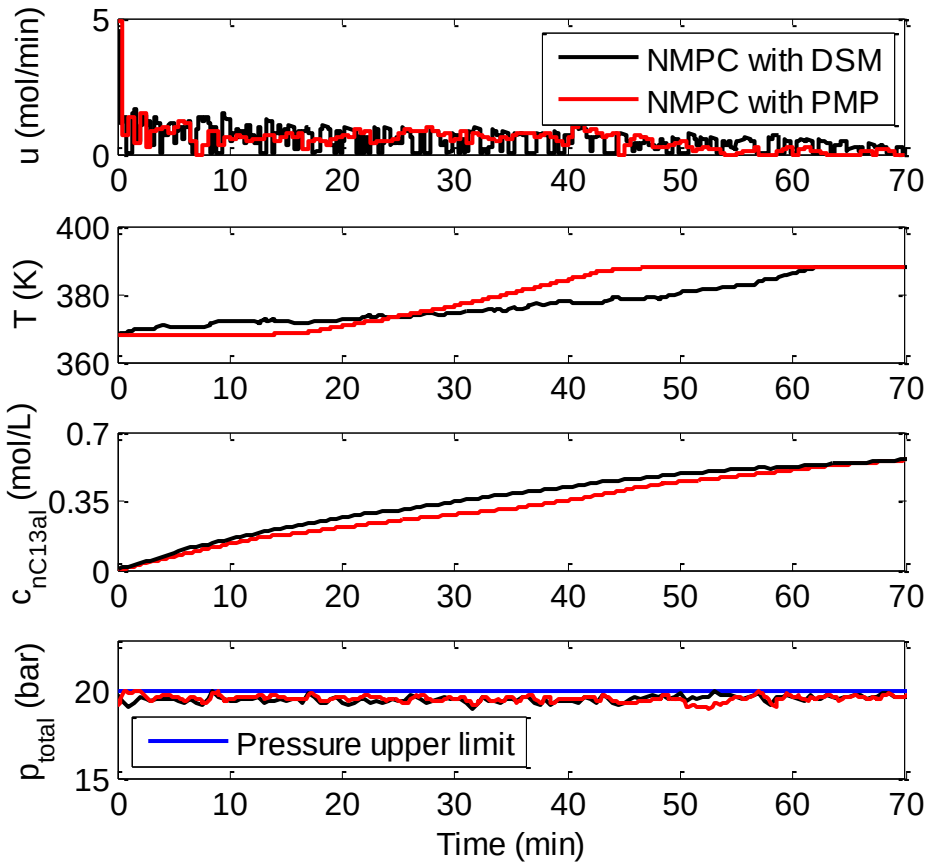

Figure 5. NMPC profiles with DSM-based and PMP-based algorithms for a particular batch and fixed final time.

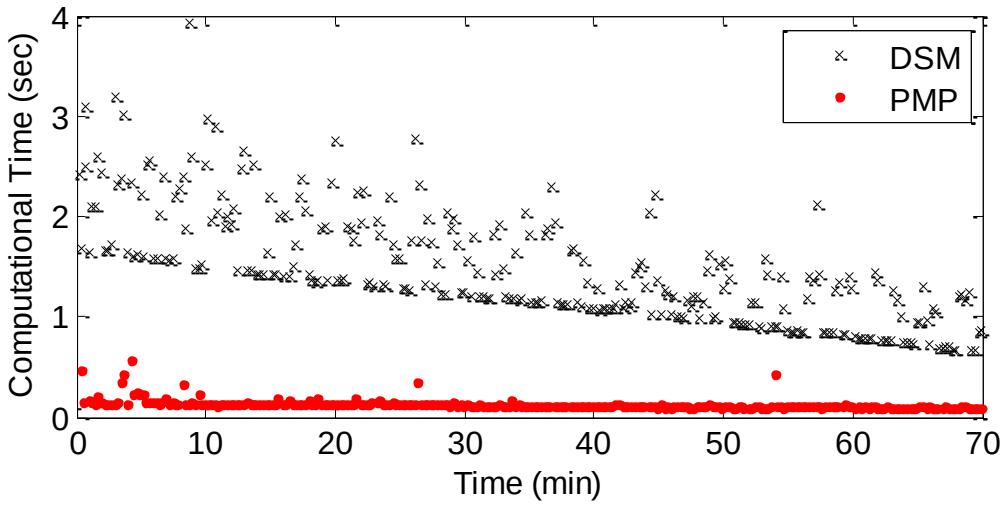

Figure 6. Computational times with DSM-based and PMP-based algorithms.

Fig. 5 shows that, with both methods, stable closed-loop performance can be achieved in the presence of parametric plant-model mismatch. In addition, the upper pressure limit is never violated thanks to the backoff term, and the rate constraint on temperature is satisfied at each NMPC iteration. Although the closed-loop input trajectories are slightly different, the optimal cost functions are very similar at the end of the batch, an indication that both methods achieve very similar performance for the maximization of nC13al. Finally, as seen in Fig. 6, PMP-based NMPC is much faster than DSM-based NMPC, especially at the beginning of the batch.

Almost 70% of the CPU time required for the PMP-based method was found to be used for integration of the states and co-states. Hence, CPU time does not decrease significantly with PMP as the horizon shrinks. Faster performance for the PMP-based method might be obtained by using fast integration algorithms or discretization methods. However, the speed and the performance of the PMP-based solution is still an open issue for large-scale systems that require high computational time for integration.

In order to test the robustness of the PMP-based NMPC, simulations were performed for 40 uncertainty realizations (Fig. 7). PMP-based NMPC is able to sustain feasible operation in all these batches in the presence of uncertainty, with a mean final nC13al concentration of 0.554 mol/L. This indicates that, under closed-loop operation, nearly 9% increase in the final amount of the desired product can be obtained compared to the infeasible (because of pressure violation) operation in Fig. 3.

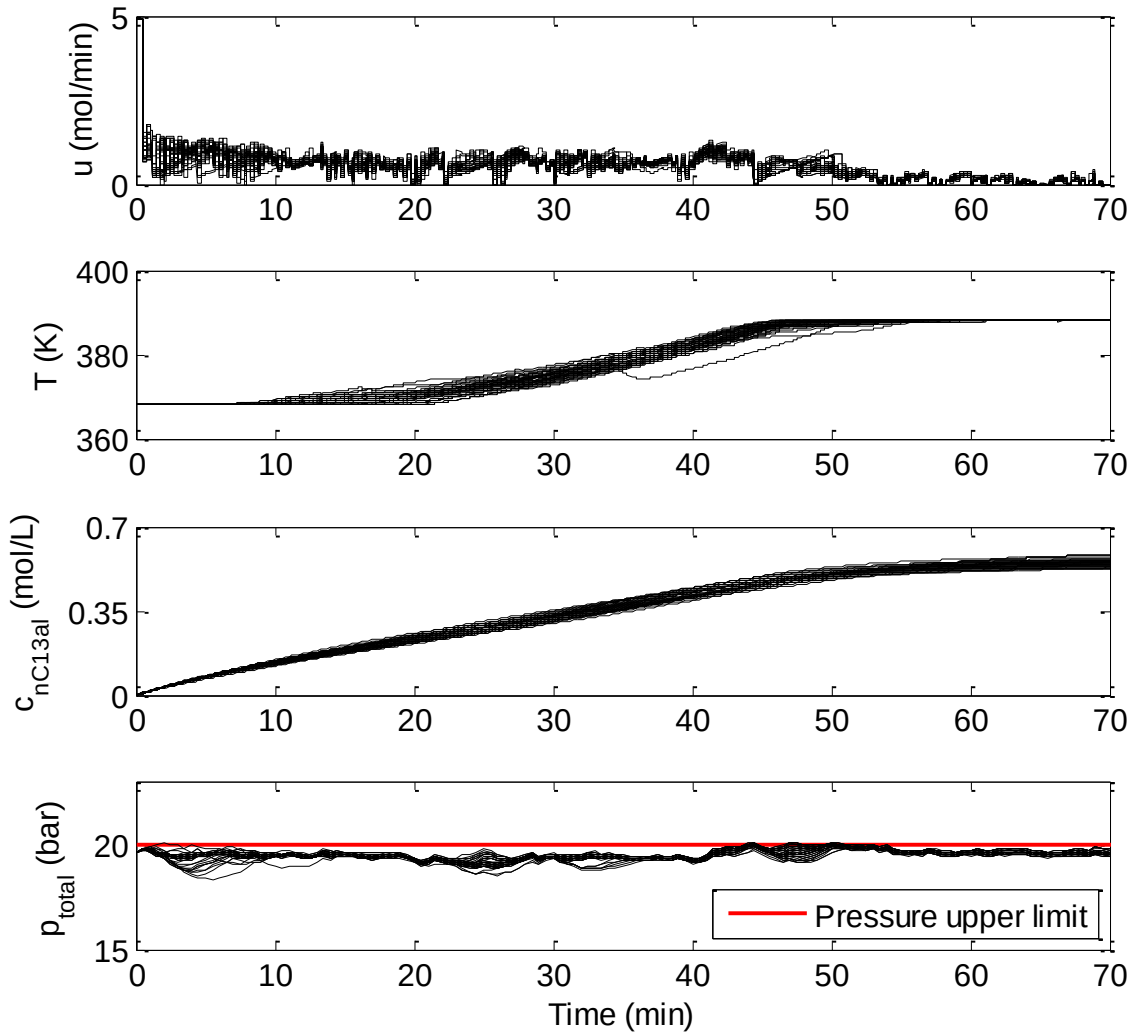

Figure 7. NMPC profiles with PMP for 40 uncertainty realizations and fixed final time.

3.4 NMPC for Batch Time Minimization

Furthermore, to check the effect of closed-loop operation on batch time reduction, the NMPC problem in Eq. 3 is reformulated such that the open-loop optimal concentration of tridecanal ($c_{nc13al}(t_f) = 0.51$ mol/L, Fig. 3b) is given as a set-point to the controller, while the final time t_f is let free. The corresponding closed-loop results for 40 different batches are given in Fig. 8.

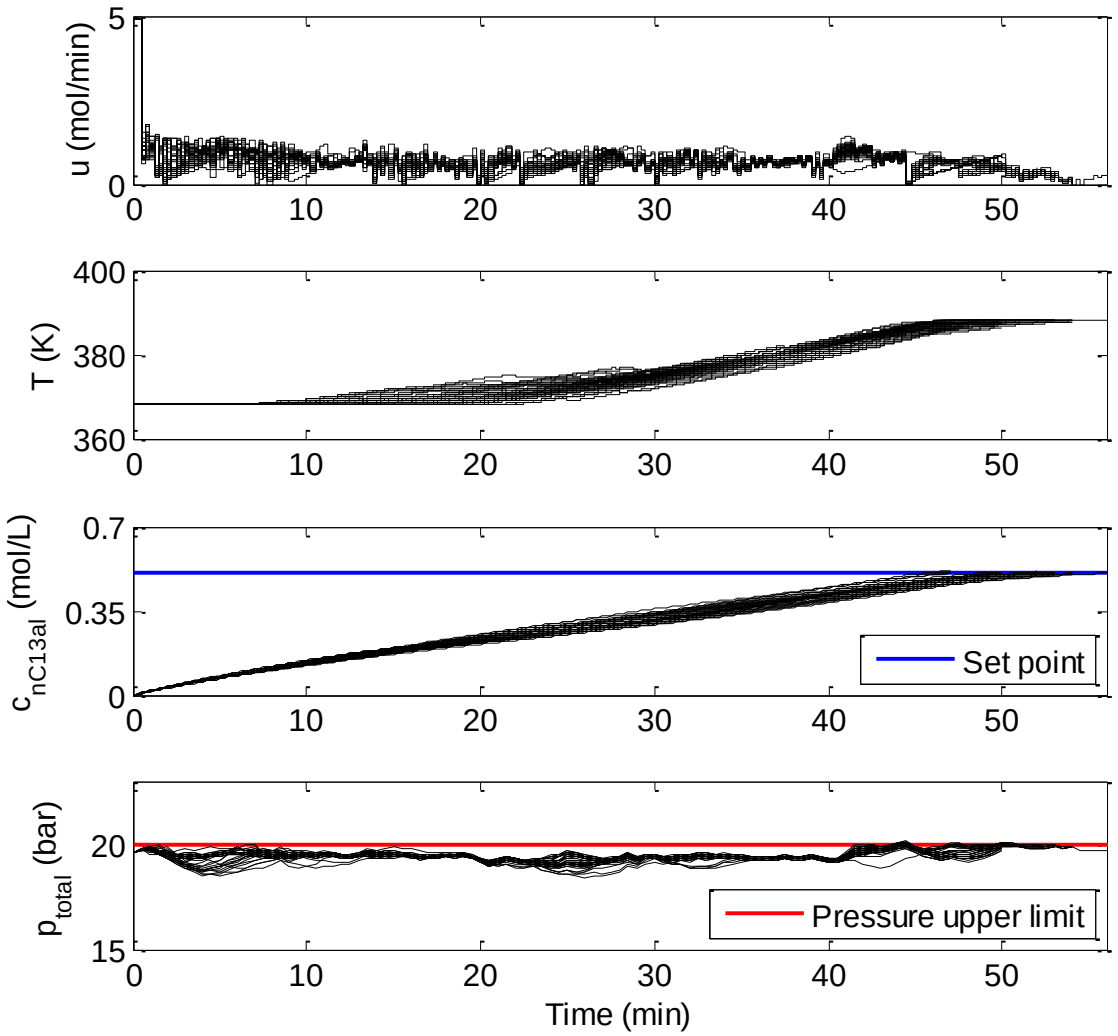

Figure 8. NMPC profiles with PMP for 40 uncertainty realizations and batch time minimization.

Fig. 8 shows that, under closed-loop operation using PMP-based NMPC, the overall batch time can be reduced from 70 to 51.36 minutes, which correspond to a 26.5% reduction (Table 3).

3.5 NMPC with Constraint Tracking

Figs. 7 and 8 illustrate that the pressure profiles are very close to the upper limit of 20 bar in all 80 batches. The optimal solution computed off-line with the nominal model also suggests that this pressure constraint is active throughout the operation (Aydin et al., 2017). Accordingly, a constraint-tracking framework can be suggested, which further reduces the computational complexity.

The feedrate of syngas u(t) is used to keep the pressure at 20 bar, while temperature T(t) is utilized to maximize the final concentration of nC13al. The control can be done implicitly with the model, that is, u(t) is computed to keep $P_{total}(t)$ constant at 20 bar or, equivalently, $\dot{p}_{total}(t) = \dot{p}_1(t) + \dot{p}_2(t) = 0$. From Eq. (3), this gives

$$u(t) = V_{liq}\left(j_1{}^{GL}(t) + j_2{}^{GL}(t)\right), \tag{5}$$

which keeps the total pressure constant. This way, $u(t)$ can be removed from the set of decision variables in Problem (3). However, $p_{total}(t)$ has to be kept constant at 20-b_s(t) bar, which is done via PID control. As seen in Fig. 9, the controller is able to keep the pressure very close to the desired value. Because the pressure limit is enforced by feedback control, a coarser input discretization can be used for the temperature (N=50 instead of N=100). The performance of NMPC with constraint tracking is shown in Fig. 9 for 40 different uncertainty realizations, with the corresponding computational times given in Fig. 10. This optimization scheme results in feasible operation, with a mean final nC13al concentration of almost 0.531 mol/L and reduced computational effort. Table 4 compares the performance of NMPC without and with constraint tracking. The introduction of constraint tracking reduces performance only by 2%.

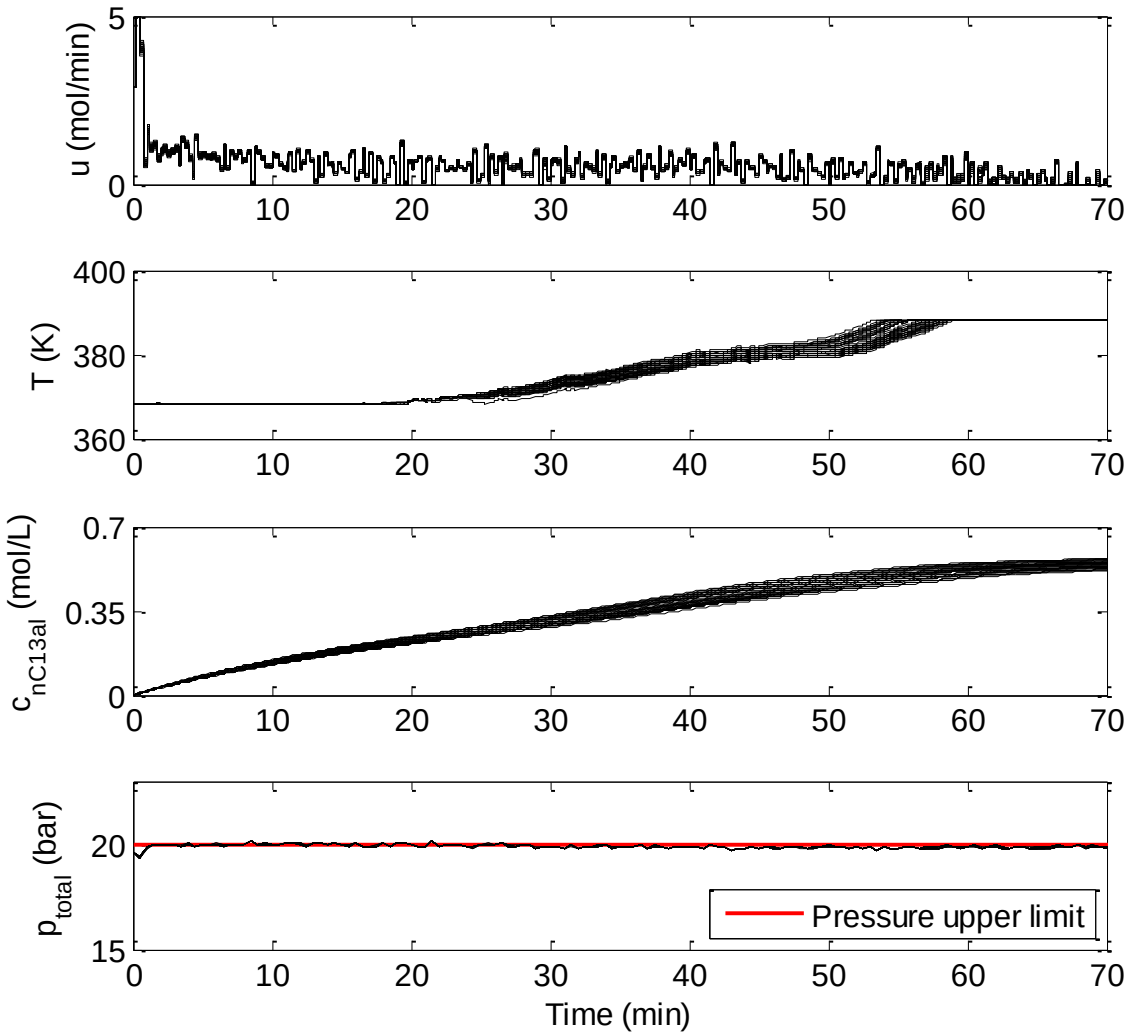

Figure 9. NMPC with constraint tracking for 40 different uncertainty realizations and fixed final time.

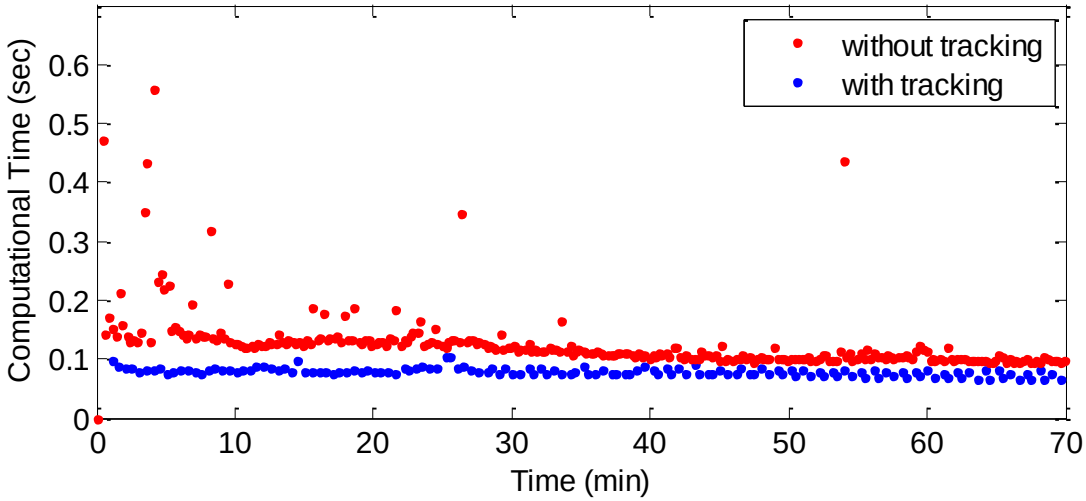

Figure 10. Computational times using PMP-based NMPC without and with constraint tracking.

Table 3. Performance of PMP-based NMPC for free final time.

Method	mean t_f for $c_{nc13al}(t_f) = 0.51$ mol/L	median t_f	st. dev. t_f
Open-loop nominal optimization (**infeasible**)	70 sec	70 sec	–
NMPC	51.36 sec	51 sec	2.28 sec

Table 4. Performance of PMP-based NMPC without and with constraint tracking for fixed final time.

Method	mean $c_{nc13al}(t_f)$	median $c_{nc13al}(t_f)$	st. dev. $c_{nc13al}(t_f)$
Open-loop nominal optimization (**infeasible**)	0.51 mol/L	0.511 mol/L	0.0126
NMPC without tracking	0.554 mol/L	0.55 mol/L	0.010
NMPC with tracking	0.543 mol/L	0.539 mol/L	0.014

4. Conclusions and Outlook

This paper has proposed an indirect PMP-based solution for shrinking-horizon NMPC and has applied it to a two-phase semi-batch hydroformylation reactor in the presence of uncertainty. A time-varying backoff approach is utilized to deal with parametric uncertainties. The pressure path constraint is indirectly adjoined into the Hamiltonian function and activated at each infeasible iteration. The computational burden stemming from the matrix factorization in large-horizon problems is reduced by the computation of states and co-states. Accordingly, the PMP-based NMPC has a computational advantage over the DSM-based NMPC, especially at the beginning of the batch. Furthermore, the PMP-based solution algorithm can be extended to track active constraints. For example, for the semi-batch hydroformylation reactor, further reduction in computational time was obtained via tracking of the active pressure constraint.

The computational speed of the PMP-based algorithms can be further increased by discretizing the state and co-state equations instead of relying on integration. Yet, it is still an open issue how the PMP-based NMPC performs for large-scale problems, where integration requires more effort. Our current interest is on testing the proposed PMP-based real-time algorithms, using on-line FTIR spectroscopy, on our mini-plant at the Max Planck Institute in Magdeburg.

Acknowledgements

This work was conducted in part in cooperation with the Collaborative Research Centre "Integrated Chemical Processes in Liquid Multiphase Systems". The financial support from the Deutsche Forschungsgemeinschaft (DFG) under the grant SFB/TRR 63 is gratefully acknowledged.

References

Abel, O., Helbig, A., Marquardt, W., Zwick, H., & Daszkowski, T. (2000). Productivity optimization of an industrial semi-batch polymerization reactor under safety constraints. Journal of Process Control, 10, 351-362.

Abel, O., & Marquardt, W. (2003). Scenario-integrated on-line optimisation of batch reactors. Journal of Process Control, 13, 703-715.

Adetola, V., & Guay, M. (2010). Integration of real-time optimization and model predictive control. Journal of Process Control, 20, 125-133.

Ali, U., & Wardi, Y. (2015). Multiple shooting technique for optimal control problems with application to power aware networks. IFAC-PapersOnLine, 48, 286-290.

Allgöwer, F., Badgwell, T. A., Qin, J. S., Rawlings, J. B., & Wright, S. J. (1999). Nonlinear predictive control and moving horizon estimation—An introductory overview. In Advances in control (pp. 391-449): Springer.

Andersson, J., & Diehl, M. (2012). Dynamic optimization with CasADi. In 51st IEEE Conference on Decision and Control (pp. 681-686).

Angeli, D., Amrit, R., & Rawlings, J. B. (2012). On average performance and stability of economic model predictive control. IEEE Transactions on Automatic Control, 57, 1615-1626.

Aydin, E., Bonvin, D., & Sundmacher, K. (2017). Dynamic optimization of constrained semi-batch processes using Pontryagin's minimum principle—An effective quasi-Newton approach. Computers & Chemical Engineering, 99, 135-144.

Biegler, L. T. (2007). An overview of simultaneous strategies for dynamic optimization. Chemical Engineering and Processing: Process Intensification, 46, 1043-1053.

Biegler, L. T., Cervantes, A. M., & Wächter, A. (2002). Advances in simultaneous strategies for dynamic process optimization. Chemical Engineering Science, 57, 575-593.

Binette, J.-C., & Srinivasan, B. (2016). On the use of nonlinear model predictive control without parameter adaptation for batch processes. Processes, 4, 27.

Bock, H. G., Diehl, M. M., Leineweber, D. B., & Schlöder, J. P. (2000). A direct multiple shooting method for real-time optimization of nonlinear DAE processes. In F. Allgöwer & A. Zheng (Eds.), Nonlinear Model Predictive Control (pp. 245-267). Basel: Birkhäuser Basel.

Bonvin, D. (1998). Optimal operation of batch reactors—A personal view. Journal of Process Control, 8, 355-368.

Bonvin, D., Srinivasan, B., & Hunkeler, D. (2006). Control and optimization of batch processes: Improvement of process operation in the production of specialty chemicals. IEEE Control Systems Magazine, 26, 34-45.

Bonvin, D., Srinivasan, B., & Ruppen, D. (2001). Dynamic optimization in the batch chemical industry. In. Preprints CPC6, Tucson, Arizona, 283–307.

Bryson, A. E. (1975). Applied Optimal Control: Optimization, Estimation and Control: CRC Press.

Cannon, M. (2004). Efficient nonlinear model predictive control algorithms. Annual Reviews in Control, 28, 229-237.

Cannon, M., Liao, W., & Kouvaritakis, B. (2008). Efficient MPC optimization using Pontryagin's minimum principle. International Journal of Robust and Nonlinear Control, 18, 831-844.

Cervantes, A., & Biegler, L. T. (1998). Large-scale DAE optimization using a simultaneous NLP formulation. AIChE Journal, 44, 1038-1050.

Cannon, M. (2004). Efficient nonlinear model predictive control algorithms. Annual Reviews in Control, 28, 229-237.

Cannon, M., Liao, W., & Kouvaritakis, B. (2008). Efficient MPC optimization using Pontryagin's minimum principle. International Journal of Robust and Nonlinear Control, 18, 831-844.

Cervantes, A., & Biegler, L. T. (1998). Large-scale DAE optimization using a simultaneous NLP formulation. AIChE Journal, 44, 1038-1050.

Chachuat, B. (2007). Nonlinear and dynamic optimization: From theory to practice. Lecture Notes.

Chachuat, B., Srinivasan, B., & Bonvin, D. (2009). Adaptation strategies for real-time optimization. Computers & Chemical Engineering, 33, 1557-1567.

De Souza, G., Odloak, D., & Zanin, A. C. (2010). Real time optimization with model predictive control. Computers & Chemical Engineering, 34, 1999-2006.

Diehl, M., Amrit, R., & Rawlings, J. B. (2011). A Lyapunov function for economic optimizing model predictive control. IEEE Transactions on Automatic Control, 56, 703-707.

Diehl, M., Bock, H. G., Diedam, H., & Wieber, P.-B. (2006). Fast direct multiple shooting algorithms for optimal robot control. In Fast Motions in Biomechanics and Robotics (pp. 65-93): Springer.

Diehl, M., Bock, H. G., Schlöder, J. P., Findeisen, R., Nagy, Z., & Allgöwer, F. (2002). Real-time optimization and nonlinear model predictive control of processes governed by differential-algebraic equations. Journal of Process Control, 12, 577-585.

Eaton, J. W., & Rawlings, J. B. (1990). Feedback control of chemical processes using on-line optimization techniques. Computers & Chemical Engineering, 14, 469-479.

Ebrahim, T., Hernandez, R., Subramanian, S., Kalliski, M., Krämer, S., & Engell, S. (2016). NCO-tracking with changing set of active constraints using multiple solution models. IFAC-PapersOnLine, 49, 79-84.

Findeisen, R., Allgöwer, F., & Biegler, L. T. (2007). Assessment and Future Directions of Nonlinear Model Predictive Control (Vol. 358): Springer.

García, C. E., Prett, D. M., & Morari, M. (1989). Model predictive control: Theory and practice—A survey. Automatica, 25, 335-348.

Hartl, R. F., Sethi, S. P., & Vickson, R. G. (1995). A survey of the maximum principles for optimal control problems with state constraints. SIAM review, 37, 181-218.

Hentschel, B., Kiedorf, G., Gerlach, M., Hamel, C., Seidel-Morgenstern, A., Freund, H., & Sundmacher, K. (2015). Model-based identification and experimental validation of the optimal reaction route for the hydroformylation of 1-dodecene. Industrial & Engineering Chemistry Research, 54, 1755-1765.

Huang, R., Biegler, L. T., & Patwardhan, S. C. (2010). Fast offset-free nonlinear model predictive control based on moving horizon estimation. Industrial & Engineering Chemistry Research, 49, 7882-7890.

Huang, R., Zavala, V. M., & Biegler, L. T. (2009). Advanced step nonlinear model predictive control for air separation units. Journal of Process Control, 19, 678-685.

Jang, H., Lee, J. H., & Biegler, L. T. (2016). A robust NMPC scheme for semi-batch polymerization reactors. IFAC-PapersOnLine, 49, 37-42.

Jung, T. Y., Nie, Y., Lee, J., & Biegler, L. (2015). Model-based on-line optimization framework for semi-batch polymerization reactors. IFAC-PapersOnLine, 48, 164-169.

Kadam, J., Schlegel, M., Srinivasan, B., Bonvin, D., & Marquardt, W. (2007). Dynamic optimization in the presence of uncertainty: From off-line nominal solution to measurement-based implementation. Journal of Process Control, 17, 389-398.

Kaiser, N. M., Flassig, R. J., & Sundmacher, K. (2016). Probabilistic reactor design in the framework of elementary process functions. Computers & Chemical Engineering, 94, 45-59.

Kameswaran, S., & Biegler, L. T. (2006). Simultaneous dynamic optimization strategies: Recent advances and challenges. Computers & Chemical Engineering, 30, 1560-1575.

Keil, F. (1999). Scientific Computing in Chemical Engineering II: Simulation, Image Processing, Optimization, and Control: Springer Science & Business Media.

Kim, N., & Rousseau, A. (2012). Sufficient conditions of optimal control based on Pontryagin's minimum principle for use in hybrid electric vehicles. Proceedings of the Institution of Mechanical Engineers, Part D: Journal of Automobile Engineering, 226, 1160-1170.

Lakshmanan, N., & Arkun, Y. (1999). Estimation and model predictive control of nonlinear batch processes using linear parameter varying models. International Journal of Control, 72, 659-675.

Li, P., Arellano-Garcia, H., & Wozny, G. (2008). Chance constrained programming approach to process optimization under uncertainty. Computers & Chemical Engineering, 32, 25-45.

Lucia, S., Finkler, T., & Engell, S. (2013). Multi-stage nonlinear model predictive control applied to a semi-batch polymerization reactor under uncertainty. Journal of Process Control, 23, 1306-1319.

Mesbah, A. (2016). Stochastic model predictive control: An overview and perspectives for future research. IEEE Control Systems Magazine, 36, 30-44.

Mesbah, A., Huesman, A. E., Kramer, H. J., Nagy, Z. K., & Van den Hof, P. M. (2011). Real-time control of a semi-industrial fed-batch evaporative crystallizer using different direct optimization strategies. AIChE Journal, 57, 1557-1569.

Mesbah, A., Streif, S., Findeisen, R., & Braatz, R. D. (2014). Stochastic nonlinear model predictive control with probabilistic constraints. In American Control Conference, 2014 (pp. 2413-2419).

Misik, S., Cela, A., & Bradac, Z. (2016). Optimal Predictive Control-A brief review of theory and practice. IFAC-PapersOnLine, 49, 324-329.

Morari, M., & Lee, J. H. (1999). Model predictive control: Past, present and future. Computers & Chemical Engineering, 23, 667-682.

Nagy, Z. K., & Braatz, R. D. (2003). Robust nonlinear model predictive control of batch processes. AIChE Journal, 49, 1776-1786.

Nagy, Z. K., Mahn, B., Franke, R., & Allgöwer, F. (2007). Real-time implementation of nonlinear model predictive control of batch processes in an industrial framework. In Assessment and Future Directions of Nonlinear Model Predictive Control (pp. 465-472): Springer.

Onori, S., Serrao, L., & Rizzoni, G. (2016). Pontryagin's Minimum Principle. In Hybrid Electric Vehicles (pp. 51-63): Springer.

Puschke, J., & Mitsos, A. (2016). Robust dynamic optimization of a semi-batch emulsion polymerization process with parametric uncertainties - A heuristic approach. IFAC-PapersOnLine, 49, 907-912.

Puschke, J., Zubov, A., Kosek, J., & Mitsos, A. (2016). Multi-model approach based on parametric sensitivities–A heuristic approximation for dynamic optimization of semi-batch processes with parametric uncertainties. Computers & Chemical Engineering.

Qin, S. J., & Badgwell, T. A. (2003). A survey of industrial model predictive control technology. Control Engineering Practice, 11, 733-764.

Rao, C. V., & Rawlings, J. B. (2002). Constrained process monitoring: Moving-horizon approach. AIChE Journal, 48, 97-109.

Rao, C. V., Rawlings, J. B., & Lee, J. H. (2001). Constrained linear state estimation—A moving horizon approach. Automatica, 37, 1619-1628.
Ruppen, D., Benthack, C., & Bonvin, D. (1995). Optimization of batch reactor operation under parametric uncertainty—Computational aspects. Journal of Process Control, 5, 235-240.
Ruppen, D., Bonvin, D., & Rippin, D. (1998). Implementation of adaptive optimal operation for a semi-batch reaction system. Computers & Chemical Engineering, 22, 185-199.
Sahinidis, N. V. (2004). Optimization under uncertainty: State-of-the-art and opportunities. Computers & Chemical Engineering, 28, 971-983.
Schäfer, A., Kühl, P., Diehl, M., Schlöder, J., & Bock, H. G. (2007). Fast reduced multiple shooting methods for nonlinear model predictive control. Chemical Engineering and Processing: Process Intensification, 46, 1200-1214.
Schneider, R., & Georgakis, C. (2013). How to not make the extended Kalman filter fail. Industrial & Engineering Chemistry Research, 52, 3354-3362.
Seki, H., Ogawa, M., Ooyama, S., Akamatsu, K., Ohshima, M., & Yang, W. (2001). Industrial application of a nonlinear model predictive control to polymerization reactors. Control Engineering Practice, 9, 819-828.
Shi, J., Biegler, L. T., Hamdan, I., & Wassick, J. (2016). Optimization of grade transitions in polyethylene solution polymerization process under uncertainty. Computers & Chemical Engineering, 95, 260-279.
Srinivasan, Bonvin, D., Visser, E., & Palanki, S. (2003). Dynamic optimization of batch processes: II. Role of measurements in handling uncertainty. Computers & Chemical Engineering, 27, 27-44.
Srinivasan, B., Biegler, L. T., & Bonvin, D. (2008). Tracking the necessary conditions of optimality with changing set of active constraints using a barrier-penalty function. Computers & Chemical Engineering, 32, 572-579.
Srinivasan, B., & Bonvin, D. (2007). Real-time optimization of batch processes by tracking the necessary conditions of optimality. Industrial & Engineering Chemistry Research, 46, 492-504.
Srinivasan, B., Palanki, S., & Bonvin, D. (2003). Dynamic optimization of batch processes: I. Characterization of the nominal solution. Computers & Chemical Engineering, 27, 1-26.
Terwiesch, P., Agarwal, M., & Rippin, D. W. (1994). Batch unit optimization with imperfect modelling: A survey. Journal of Process Control, 4, 238-258.
Valappil, J., & Georgakis, C. (2002). Nonlinear model predictive control of end-use properties in batch reactors. AIChE Journal, 48, 2006-2021.
Vassiliadis, V. S., Sargent, R. W. H., & Pantelides, C. C. (1994). Solution of a class of multistage dynamic optimization problems. 2. Problems with path constraints. Industrial & Engineering Chemistry Research, 33, 2123-2133.
Visser, E., Srinivasan, B., Palanki, S., & Bonvin, D. (2000). A feedback-based implementation scheme for batch process optimization. Journal of Process Control, 10, 399-410.
Wächter, A., & Biegler, L. T. (2006). On the implementation of an interior-point filter line-search algorithm for large-scale nonlinear programming. Mathematical Programming, 106, 25-57.
Welz, C., Srinivasan, B., & Bonvin, D. (2008). Measurement-based optimization of batch processes: Meeting terminal constraints on-line via trajectory following. Journal of Process Control, 18, 375-382.
Zavala, V. M., & Biegler, L. T. (2009). The advanced-step NMPC controller: Optimality, stability and robustness. Automatica, 45, 86-93.

Zhang, S., Xiong, R., & Sun, F. (2017). Model predictive control for power management in a plug-in hybrid electric vehicle with a hybrid energy storage system. Applied Energy, 185, Part 2, 1654-1662.